ON THE CONSTRUCTION OF VIRTUAL INTERIOR POINT SOURCE TRAVEL TIME DISTANCES FROM THE HYPERBOLIC NEUMANN-TO-DIRICHLET MAP

MAARTEN V. DE HOOP [†], PAUL KEPLEY [‡], AND LAURI OKSANEN [§]

Abstract. We introduce a new algorithm to construct travel time distances between a point in the interior of a Riemannian manifold and points on the boundary of the manifold, and describe a numerical implementation of the algorithm. It is known that the travel time distances for all interior points determine the Riemannian manifold in a stable manner. We do not assume that there are sources or receivers in the interior, and use the hyperbolic Neumann-to-Dirichlet map, or its restriction, as our data. Our algorithm is a variant of the Boundary Control method, and to our knowledge, this is the first numerical implementation of the method in a geometric setting.

Key words. Boundary Control method, travel time distances, wave equation

AMS subject classifications. 35R30, 35L05

1. Introduction. We consider the inverse boundary value problem for the acoustic wave equation on a domain in $\mathbb{R}^n$, or Riemannian manifold with boundary, M. The problem is to recover, in an appropriate region near ∂M and appropriate coordinates, a spatially varying wave speed c or metric g, from the Neumann-to-Dirichlet map or its restriction to a subset of the boundary, say $\Gamma \subset \partial M$.

Waves propagate in a domain M with speed c, and the travel time for a wave between a pair of points x and y in M is given by the Riemannian distance $d(x, y)$ computed with respect to the travel time metric $c^{-2}dx^2$. For this reason, it is natural to formulate the inverse boundary value problem using concepts from Riemannian geometry. Also, this allows us to consider anisotropic wave speeds in a unified way.

We present a new method to use the restriction of the Neumann-to-Dirichlet map to determine travel time distances of the form $d(x, y)$ where $y \in \Gamma$ and x belongs to a semi-geodesic neighborhood of Γ. That is, y is a point in the set where we have boundary measurements, and $x \in M$ belongs to a region near Γ where the semi-geodesic coordinates of Γ are valid (see Section 2.2 for definitions). The precise subset of M for which we can determine travel times depends upon the data and the geometry of M, however we remark that this subset is not necessarily a thin layer about Γ. We refer to these travel times as *point source travel time data*, since the distance $d(x, y)$ corresponds to the first arrival travel time from a (virtual) interior point source located at x as recorded at the boundary at y. We emphasize that our method synthesizes the travel times from a point source in the interior of M without requiring an actual receiver or source at that location.

To motivate our results, we note that for a Riemannian manifold with boundary

---

(M, g), the set of travel times $\{d(x, y) : x \in M, y \in \partial M\}$ have previously been shown to determine the geometry of M, see e.g. [19]. In particular, in the full boundary data case, it has been shown that this determination is even stable [20]. Furthermore, it can be shown that travel times determine shape operators that appear as data for the generalized Dix method [14]. This is of particular interest in the isotropic case, since that method allows for the local nonlinear reconstruction of a wave speed near geodesic rays. We also note that in [33], an explicit reconstruction method is developed for conformally Euclidean metrics, wherein travel times for points in a semi-geodesic neighborhood of Γ and properties of Killing vector fields are used to determine the metric in the same neigborhood in Euclidean coordinates.

Our method to determine boundary distances works by first using a variant of the Boundary Control method (BC method) to determine volumes of subdomains of M referred to as wave caps. These volumes are computed by solving a collection of regularized ill-posed linear problems. The BC method originates from [6], where it was used to solve the inverse boundary value problem for the acoustic wave equation. We note that [8] was the first variant of the BC method posed in a geometric setting. For a thorough overview of the BC method, we refer to [19] and [7]. Regularization theory was first combined with the BC method in [10], and the technique used, here, to determine volumes was developed in [28].

In the present paper, we introduce a procedure that uses volumes of wave caps to construct point source travel time data for points near Γ. This, in turn, reduces the inverse boundary value problem to the stable problem of determining a Riemannian submanifold of (M, g) near Γ from point source travel time data. In particular, our procedure splits the inverse boundary value problem into an ill-posed but linear step (the volume computation) and a non-linear but well-posed step (distance determination and reconstruction of the submanifold).

We describe a numerical implementation of our method, and provide computational experiments to demonstrate our technique. We remark that our computational experiments provide the first computational realization of a geometric variant of the BC method. Moreover, we explain how the instability of the volume computation step is manifest in our computational experiments. All variants of the BC method that use partial data contain similar unstable components, and we believe that the instability of the method reflects the ill-posedness of the inverse boundary value problem itself. However, contrary to Calderón's problem, that is, the elliptic inverse boundary value problem [12, 37], it is an open question whether the inverse boundary value problem for the wave equation is ill-posed in general. For results concerning the stability of Calderón's problem we refer to [1, 26].

Also, we point out that under favorable geometric assumptions, the hyperbolic inverse boundary value problem is known to have better stability properties than Calderón's problem, see e.g. [9, 24, 27, 34, 35, 36] and references therein. These results assume data on the whole boundary or that Γ is strictly convex.

2. Statement of the results. In this section, we describe our data and assumptions, and what we intend to recover from the data.

2.1. Direct problem as a model for measurements. We work in the following setting,

ASSUMPTION 1. *M is a smooth compact connected manifold with smooth boundary ∂M, and g is an unknown smooth Riemannian metric on M.*

Let $\mu \in C^\infty(\overline{M})$ be a strictly positive weight function, note that we do not require any additional information about μ. We consider the following wave equation on (M, g) with boundary source $f \in C_0^\infty((0, \infty) \times \partial M)$,

(1)
$$\begin{aligned}
\partial_t^2 u(t, x) - \Delta_{g,\mu} u(t, x) &= 0, & (t, x) &\in (0, \infty) \times M, \\
N_\mu u(t, x) &= f(t, x), & (t, x) &\in (0, \infty) \times \partial M \\
u(0, \cdot) = 0, \quad \partial_t u(0, \cdot) &= 0, & x &\in M.
\end{aligned}$$

The operator $\Delta_{g,\mu}$ is the weighted Laplace-Beltrami operator, which is given by $\Delta_{g,\mu} w(x) := \mu^{-1} \operatorname{div}_g(\mu \operatorname{grad}_g w)$ and $N_\mu w := -\mu \langle \nu, \operatorname{grad}_g w \rangle_g$ is the associated Neumann derivative. Here, ν is the inward pointing unit normal vector to ∂M in the metric g, div_g and grad_g are respectively the divergence and gradient on (M, g), and $\langle \cdot, \cdot \rangle_g$ denotes the inner product with respect to the metric g. We remark that $\Delta_{g,\mu}$ is defined so that we can also handle the usual acoustic wave equation. Indeed, if $M \subset \mathbb{R}^n$ is a domain equipped with a strictly positive wave speed $c \in C^\infty(\overline{M})$, then with respect to the conformally Euclidean metric $g = c^{-2} dx^2$, the weight $\mu = c^{n-2}$ yields $\Delta_{g,\mu} = c^2 \Delta$, where Δ denotes the Euclidean Laplacian.

We now introduce our data model. We denote the solution to (1) with Neumann boundary source f by $u^f(t, x)$. For $T > 0$, and $\Gamma \subset \partial M$ an open set, we define the Neumann-to-Dirichlet operator associated with (1) by,

$$\Lambda_\Gamma^{2T} : f \mapsto u^f|_{(0,2T) \times \Gamma}, \quad f \in C_0^\infty((0, 2T) \times \Gamma).$$

Note that we are identifying functions in $[0, 2T] \times \Gamma$ with their zero continuations in $[0, 2T] \times \partial M$, and we will continue to do this. The map Λ_Γ^{2T} extends to a bounded operator on $L^2((0, 2T) \times \Gamma)$, see for instance [22]. For data, we suppose that Λ_Γ^{2T} is known. We note that Λ_Γ^{2T} models boundary measurements for waves generated with acoustic sources and receivers located on Γ, where the waves are both generated and recorded on Γ for $2T$ units of time. In addition, we note that in seismic applications the Neumman-to-Dirichlet map appears in simultaneous source acquisition.

Our primary interest is in constructing distances with respect to the Riemannian metric g, and we denote the Riemannian distance between the points $x, y \in M$ by $d(x, y)$. To simplify our distance computation procedure, we assume:

ASSUMPTION 2. *The distances $d(y, z)$ are known for $y, z \in \Gamma$ with $d(y, z) < T$.*

We note that this is not a major limitation since for $y, z \in \Gamma$ with $d(y, z) < T$, the data Λ_Γ^{2T} determines $d(y, z)$, see e.g. [13, Section 2.2].

2.2. Construction of the point source travel time data. We define $R(M)$ to be the set of *boundary distance functions* on M,

(2)
$$R(M) = \{r_x : x \in M, \text{ and for } z \in \partial M, \ r_x(z) := d(x, z)\}.$$

We note that, for $x \in M$ and $z \in \partial M$, $r_x(z)$ gives the minimum travel time from x to z. With this interpretation, $r_x(z)$ represents the first arrival time at z from a wave generated by a point source located at x.

In Section 3 we develop a method to synthesize values of r_x from Λ_Γ^{2T} for points x that are sufficiently near Γ, and which are indexed by a set of coordinates known as semi-geodesic coordinates[1]. We refer to this procedure as forming *point source travel*

---

[1]Such coordinates are considered in seismology, where they are referred to as image ray coordinates [17].

time data, since our procedure reproduces the travel time information for a point source located at x without having a source or receiver there.

The geometry of the supports of solutions to (1) inform our constructions. To be explicit, let τ be a function on Γ satisfying $0 \leq \tau(z) \leq T$ for all $z \in \Gamma$ and define the *domain of influence* of τ,

$$M(\tau) := \left\{ x \in M \; : \; \text{there exists a } z \in \bar{\Gamma} \text{ such that } d(x, z) \leq \tau(z) \right\}.$$

We depict $M(\tau)$ in Figure 1a. Consider the set

(3) $$S_\tau := \{(t, z) \in (0, T) \times \bar{\Gamma} : \; t \in (T - \tau(z), T)\}.$$

We recall that solutions to (1) exhibit finite speed of propagation in the metric g, and specifically, if $\text{supp}(f) \subset S_\tau$ then $\text{supp}(u^f(T, \cdot)) \subset M(\tau)$.

When τ is a multiple of an indicator function, we will occasionally use a special notation for $M(\tau)$. To be specific, we denote the indicator function of a set S by 1_S, and for $s \geq 0$ we will use the notation $M(\Gamma, s) := M(s 1_\Gamma)$ and $M(y, s) := M(s 1_{\{y\}})$.

We denote the unit sphere bundle $SM := \{\xi \in TM : \; |\xi|_g = 1\}$, and define the inward/outward pointing sphere bundles by $\partial_\pm SM := \{\xi \in \partial SM : \; (\xi, \pm \nu)_g > 0\}$, where ν is the inner unit normal vector field on ∂M. We define the *exit time* for $(x, \xi) \in SM \setminus \overline{\partial_+ SM}$, by $\tau_M(x, \xi) := \inf\{s \in (0, \infty) : \; \gamma(s; x, \xi) \in \partial M\}$ where $\gamma(\cdot; x, \xi)$ is the geodesic with the initial data $\gamma(0) = x$, $\dot{\gamma}(0) = \xi$.

For $y \in \Gamma$ we define $\sigma_\Gamma(y)$ to be the maximal arc length for which the normal geodesic beginning at y minimizes the distance to Γ. That is,

$$\sigma_\Gamma(y) := \max\{s \in (0, \tau_M(y, \nu)] : \; d(\gamma(s; y, \nu), \Gamma) = s\}.$$

We recall, see e.g. [19, p. 50] that $\sigma_\Gamma(y) > 0$ for $y \in \Gamma$. Moreover, σ_Γ is lower semi-continuous, see e.g. [23, Lemma 12]. We define

(4) $$x(y, s) := \gamma(s; y, \nu) \quad \text{for } y \in \Gamma \text{ and } 0 \leq s < \sigma_\Gamma(y).$$

The mapping $(y, s) \mapsto x(y, s)$ is a diffeomorphism from $\{(y, s) : y \in \Gamma, 0 \leq s < \sigma_\Gamma(y)\}$ onto its image, so we will refer to (y, s) as semi-geodesic coordinates for $x(y, s)$. This is a slight abuse of terminology, since the pair (y, s) belongs to $\Gamma \times [0, \infty)$ instead of a subset of $\mathbb{R}^n$. On the other hand, by selecting local coordinates on Γ these "coordinates" can be made into legitimate coordinates.

Next, we recall the definition of the *cut locus* of Γ, which is the set of points given by $\mathcal{C} = \{x(y, \sigma_\Gamma(y)) : \; y \in \Gamma\}$. We depict $\mathcal{C}$ in Figure 1b. Due to the lower semi-continuity of σ_Γ and boundedness of Γ, the distance between Γ and $\mathcal{C}$ is positive.

We will use the following notions of volume: let dV_g and dS_g denote the Riemannian volume densities of (M, g) and $(\partial M, g|_{\partial M})$ respectively. We remark that dS_g is determined on Γ by Λ_Γ^{2T}, see e.g. [13, Section 2.2] so we assume that it is known. We define the natural Riemannian volume density associated with $\Delta_{g,\mu}$ by $dV_\mu := \mu dV_g$. We remark that its name derives from the fact that $\Delta_{g,\mu}$ is self-adjoint on $L^2(M; dV_\mu)$ with domain $H_0^1(M) \cap H^2(M)$. The volume density dV_μ determines a volume measure which we denote Vol_μ. In addition, we will use the following shorthand notation for volumes of domains of influence $m(\tau) := \text{Vol}_\mu(M(\tau))$.

We now describe a set of geometrically relevant subsets whose volumes will allow us to determine distances. Let $y \in \Gamma$, and let $s, h > 0$ satisfy $s + h < \sigma_\Gamma(y)$. We define the *wave cap*,

$$\text{cap}_\Gamma(y, s, h) := M(y, s + h) \setminus M^\circ(\Gamma, s),$$
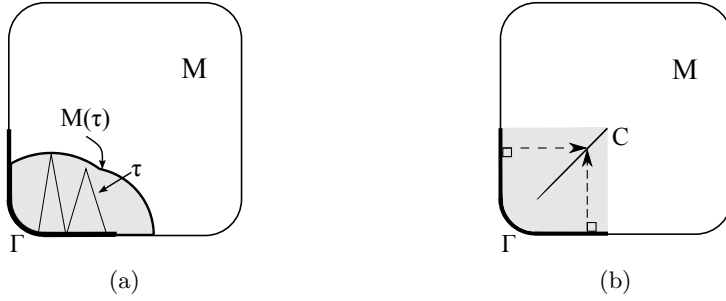
Fig. 1: (a) The domain of influence for a τ in $C(\overline{\Gamma})$ along with the profile of τ. (b) The cut locus of Γ along with a pair of equal length geodesics showing the break-down of the semi-geodesic coordinates at $\mathcal{C}$. The shaded region is the subset of M that supports semi-geodesic coordinates.

where $M^\circ(\Gamma, s) = \{x \in M : d(x, \Gamma) < s\}$. Note that under the above hypotheses, $x(y, s)$ belongs to $\mathrm{cap}_\Gamma(y, s, h)$. We will use wave cap volumes to determine distances.

Our main result is an algorithm to use the data Λ_Γ^{2T} to construct distances of the form $r_{x(y,s)}(z)$ for $y, z \in \Gamma$ and $s > 0$ with $d(x(y, s), z) < \min(\sigma_\Gamma(y), T)$. Our procedure can also be viewed as a constructive proof of the following known result, see e.g. [19]:

THEOREM 1. *Let $y, z \in \Gamma$ and $s > 0$ with $d(x(y, s), z) < \min(\sigma_\Gamma(y), T)$. Then Λ_Γ^{2T} determines $r_{x(y,s)}(z)$.*

The constructive proof will be given in Section 4. We note that this construction can also be viewed as a series of experiments. Following the proofs in Section 4.2, we provide an algorithmic overview of our distance computation procedure.

3. The Boundary Control method. In this section, we describe the elements of the BC method required to determine $m(\tau)$ from Λ_Γ^{2T}. In addition, we briefly contrast our technique to alternative approaches to the BC method, and provide an overview of some computational aspects of the BC method.

The purpose of the BC method is to gain information about the interior of M by processing boundary measurements for waves that propagate in M. To begin, we recall the *control map*, W_τ, which takes a Neumann boundary source f to the corresponding solution at time T. That is, let $\tau : \overline{\Gamma} \to [0, T]$ be continuous or a linear combination of characteristic functions of open sets and define,

$$W_\tau f := u^f(T, \cdot), \quad W_\tau : L^2(S_\tau) \to L^2(M).$$

The map W_τ is continuous, compact even, as a map from $L^2(S_\tau)$ into $L^2(M)$, see e.g. [22, 39]. We will write $W := W_\tau$ in the special case that $\tau \equiv T$, and we note that in this case, $S_\tau = (0, T) \times \Gamma$. Thus, for any other $\tau : \Gamma \to [0, T]$, W_τ can be viewed as a restriction of W to sources supported in S_τ.

One cannot directly observe the output of W_τ from boundary measurements because its output is a wave in the interior of M. Thus, in order to deduce information about the interior of M, one forms the *connecting operator*,

$$K_\tau := W_\tau^* W_\tau, \quad K : L^2(S_\tau) \to L^2(S_\tau).$$

The continuity of W_τ implies that K_τ is a continuous operator on $L^2(S_\tau)$. The practical utility of K_τ is that it can be computed by processing the boundary data, Λ_Γ^{2T}, see (6) below. This fact was first observed by Blagoveschenskii in the 1+1-dimensional case [11]. We remark that K_τ derives its name from the fact that it connects the inner product on boundary sources with the inner product on waves in the interior. That is, for f, h in $C_0^\infty(S_\tau)$,

$$(5) \qquad \langle u^f(T, \cdot), u^h(T, \cdot) \rangle_{L^2(M; dV_\mu)} = \langle f, Kh \rangle_{L^2(S_\tau; dt \otimes dS_g)}.$$

We next recall the "Blagoveschenskii Identity," which gives an expression for K_τ in terms of the data Λ_Γ^{2T}. In particular, we use the expression for K_τ used in [30],

$$(6) \qquad K_\tau = P_\tau \left(J\Lambda_\Gamma^{2T}\Theta - R\Lambda_\Gamma^T RJ\Theta \right) P_\tau.$$

Here, $\Theta : L^2((0, T) \times \Gamma) \to L^2((0, 2T) \times \Gamma)$ is the inclusion (zero padding) given by:

$$\Theta f(t, \cdot) := \begin{cases} f(t, \cdot) & 0 < t \leq T, \\ 0 & T < t < 2T, \end{cases}$$

$R : L^2((0, T) \times \Gamma) \to L^2((0, T) \times \Gamma)$ is the time reversal on $(0, T)$ given by:

$$Rf(t, \cdot) := f(T - t, \cdot) \quad 0 < t < T,$$

$J : L^2((0, 2T) \times \Gamma) \to L^2((0, T) \times \Gamma)$ is the time integration, given by:

$$Jf(t, \cdot) := \frac{1}{2} \int_t^{2T-t} f(s, \cdot) \, ds \quad 0 < t < T,$$

and $P_\tau : L^2((0, T) \times \Gamma) \to L^2((0, T) \times \Gamma)$ is the orthogonal projection onto $L^2(S_\tau)$ given by:

$$(7) \qquad P_\tau f := 1_{S_\tau} \cdot f.$$

We will use the special notation $K := K_\tau$ when $\tau \equiv T$. In this case, the operator P_τ coincides with the identity and (5) can be written as $K = J\Lambda_\Gamma^{2T}\Theta - R\Lambda_\Gamma^T RJ\Theta$. Thus, for any τ, the operator K_τ can be expressed as $K_\tau = P_\tau K P_\tau$.

3.1. Overview of BC method variants. There are several variants of the BC method, all of which are based on solving control problems of the form: Given a function ϕ on M, and a function $\tau : \overline{\Gamma} \to [0, T]$, find a boundary source f such that

$$(8) \qquad W_\tau f = \phi.$$

In general, this problem is not solvable since the range of W_τ is generally not closed. On the other hand, it can be shown that *approximate controllability* holds, that is, there is a sequence $(f_j)_{j=1}^\infty \subset C_0^\infty(S_\tau)$ such that

$$(9) \qquad \lim_{j \to \infty} W_\tau f_j = 1_{M(\tau)}\phi, \quad \text{in } L^2(M).$$

The approximate controllability follows from the hyperbolic unique continuation result by Tataru [38] by a duality argument, see e.g. [19, p. 157].

The original version of the BC method [6] uses the Gram-Schmidt orthonormalization to find a sequence $(f_j)_{j=1}^\infty$ satisfying (9). The method was implemented

numerically in [5], and it requires choosing an initial system of boundary sources, see step 2 in [5, p. 233]. No constructive way to choose the initial boundary sources is given, and some choices may lead to an ill-conditioned orthonormalization process, see the discussion in [10].

More recently, Bingham, Kurylev, Lassas and Siltanen introduced a variant of the BC method where the Gram-Schmidt process is replaced by a quadratic optimization [10]. Their method is posed in the case $\Gamma = \partial M$, and is based on constructing a sequence $(f_j)_{j=1}^\infty$ such that the limit (9) becomes focused near a point. To elaborate, their method considers an arbitrary $h \in L^2((0,T) \times \partial M)$ with ϕ chosen as $\phi = Wh$. For a point $y \in \partial M$ and small enough $0 < s, r < T$, they choose appropriate τ to produce a sequence of sources $(f_j)_{j=1}^\infty \subset S_\tau$ such that $Wf_j \to 1_{\mathrm{cap}_{\partial M}(y,s,r)} Wh$. However, no constructive procedure to choose the boundary source h is given, and some choices may lead to sequences such that this limit vanishes also near the point where it should be focused, see the assumption on the non-vanishing limit in [10, Corollary 2]. We note that the method [10] has not been implemented numerically.

Our approach employs a quadratic optimization similar to [10] but differs from it by selecting $\phi = 1$ in place of Wh. By solving the approximate control problems for this choice of ϕ, we can compute volumes $m(\tau)$ for certain functions $\tau : \overline{\Gamma} \to [0,T]$. We note that the method we use to compute these volumes was developed in [28, 29], and it was applied to an inverse obstacle problem in [30]. Here we show how to compute the boundary distance functions from the volumes $m(\tau)$.

Our method contains only constructive choices of boundary sources, and it allows us to understand the numerical errors that we make in each step of the algorithm. In Section 5, we see that the dominating source of error in our computational experiments is related to the instability of the control problem (8) under the constraint $\mathrm{supp}(f) \subset S_\tau$. This instability is inherent in all the variants of the BC method mentioned above.

In addition to [5], the only multidimensional implementations of a variant of the BC method, that we are aware of, are [31, 32]. These variants are based on solving the control problem (8) without the constraint $\mathrm{supp}(f) \subset S_\tau$. The target function ϕ is chosen to be harmonic, and the method exploits the density of products of harmonic functions in $L^2(M)$. Such an approach works only in the isotropic case, that is, for the wave equation $\partial_t^2 - c(x)^2 \Delta$ where the wave speed $c(x) > 0$ is scalar valued.

We also mention that the original version of the BC method [6] assumes the wave equation to be isotropic, and that in [24], an approach similar to [32] was shown to recover a lowpass version of the wave speed in a Lipschitz stable manner under additional geometric assumptions. Furthermore, we refer to [18] for a comparison of the BC method and other inversion methods in the 1+1-dimensional case.

3.2. Regularized estimates of volumes of domains of influence. We now explain how we pose our approximate control problems, and how we use their solutions to compute volumes of domains of influence. To begin, let $\tau : \overline{\Gamma} \to [0,T]$ be either a linear combination of characteristic functions of open sets or $\tau \in C(\overline{\Gamma})$. We obtain an approximate solution to (8) with right-hand side $\phi = 1$, by solving the following minimization problem: for $\alpha > 0$ let

$$(10) \qquad f_\alpha := \operatorname*{argmin}_{f \in L^2(S_\tau)} \|u^f(T, \cdot) - 1\|_{L^2(M;dV_\mu)}^2 + \alpha \|f\|_{L^2(S_\tau;dt \otimes dS_g)}^2.$$

As was shown in [28], for τ as above: this problem is solvable, the solution can be obtained by solving a linear problem involving K_τ, and $u^{f_\alpha}(T, \cdot) \to 1_{M(\tau)}$ as $\alpha \to 0$. For the convenience of the reader, we outline the proof here, and moreover, we recall that the approximate control solutions, f_α, can be used to compute $m(\tau)$.

To show that (10) has a solution we first recall two results about Tikhonov regularization. For proofs see e.g. [21, Th. 2.11] and [30], respectively.

LEMMA 2. *Suppose that X and Y are Hilbert spaces. Let $y \in Y$ and let $A : X \to Y$ be a bounded linear operator. Then for all $\alpha > 0$ there is a unique minimizer of*

$$\|Ax - y\|^2 + \alpha \|x\|^2$$

given by $x_\alpha = (A^*A + \alpha)^{-1}A^*y$.

LEMMA 3. *Suppose that X and Y are Hilbert spaces. Let $y \in Y$ and let $A : X \to Y$ be a bounded linear operator with range $R(A)$. Then $Ax_\alpha \to Qy$ as $\alpha \to 0$, where $x_\alpha = (A^*A + \alpha)^{-1}A^*y$, $\alpha > 0$, and $Q : Y \to \overline{R(A)}$ is the orthogonal projection.*

Since W_τ is bounded, the first Lemma implies that (10) is solvable. To apply the second lemma to our current setting, we must describe the range of W_τ and compute $W_\tau^* 1$. Toward that end, we recall that $\text{supp}(W_\tau f) \subset M(\tau)$ by finite speed of propagation. When τ is a linear combination of characteristic functions of open sets, Tataru's unique continuation [38] implies that the inclusion

$$(11) \qquad \{W_\tau f; \ f \in L^2(S_\tau)\} \subset L^2(M(\tau)),$$

is dense, see e.g. [19, Th. 3.10]. The result was extended to the case of $\tau \in C(\overline{\Gamma})$ in [28]. Thus $\overline{R(W_\tau)} = L^2(M(\tau))$ for the functions τ under consideration. To compute $W_\tau^* 1$, we note an equality similar to (5) that is satisfied for $f \in L^2(S_\tau)$:

$$(12) \qquad \langle u^f(T, \cdot), 1 \rangle_{L^2(M; dV_\mu)} = \langle f, P_\tau b \rangle_{L^2((0,T) \times \partial M; dt \otimes dS_g)}.$$

Here, P_τ is defined by (7), and $b(t, x) := T - t$ for $(t, x) \in (0, T) \times \Gamma$. Thus, $W_\tau^* 1 = P_\tau b$.

Applying Lemmas 2 and 3 to the observations above, we see that for each $\alpha > 0$, equation (10) has a unique solution f_α, given by:

$$(13) \qquad f_\alpha := (W_\tau^* W_\tau + \alpha)^{-1} W_\tau^* 1 = (K_\tau + \alpha)^{-1} P_\tau b,$$

thus f_α is obtained from the data. Moreover, the waves $W_\tau f_\alpha$ satisfy $W_\tau f_\alpha \to Q_\tau 1$ in $L^2(M)$ as α tends to zero, where Q_τ is the projection of $L^2(M)$ onto the subspace $\overline{R(W_\tau)} = L^2(M(\tau))$. Note that $Q_\tau 1 = 1_{M(\tau)}$. Using this fact and applying (12) to f_α we conclude,

$$(14) \qquad m(\tau) = \lim_{\alpha \to 0+} \langle f_\alpha, P_\tau b \rangle_{L^2((0,T) \times \partial M; dt \otimes dS_g)}.$$

Thus we can compute $m(\tau)$ from operations performed on the data Λ_Γ^{2T}.

4. Constructing distances. In this section, we present our proof of Theorem 1. We accomplish this through a sequence of lemmas that are designed to illuminate the steps required to turn the theorem into an algorithm. Also, we provide an alternative technique to determine distances, which we use in our numerical implementation.

4.1. Constructive proof of Theorem 1. The following lemma provides a bound on the distance between a point and a wave cap,

LEMMA 4. *Let $y \in \Gamma$, $s \in (0, \sigma_\Gamma(y))$, and $h \in (0, \sigma_\Gamma(y) - s)$. Let $z \in \Gamma$ and $r > 0$. Then $d(z, \text{cap}_\Gamma(y, s, h)) < s + r$ if and only if*

$$(15) \qquad m(s1_\Gamma + r1_z + h1_y) - m(s1_\Gamma + r1_z) < m(s1_\Gamma + h1_y) - m(s1_\Gamma).$$

We note that (15) tests whether there is an overlap between the sets $\text{cap}_\Gamma(y, s, h)$ and $\text{cap}_\Gamma(y, s, r)$, see Figure 2.

Proof. Since $h > 0$ and $h < \sigma_\Gamma(y) - s$, we see that $\mathrm{cap}_\Gamma(y, s, h)$ contains a non-empty open set. In particular, it has strictly positive measure. Moreover, if $d(z, \mathrm{cap}_\Gamma(y, s, h)) < s + r$ then the intersection of $\mathrm{cap}_\Gamma(y, s, h)$ and $M(z, s+r)$ contains a non-empty open set and has strictly positive measure.

We note that $m(s1_\Gamma + h1_y)$ is the measure of $M(y, s+h) \cup M(\Gamma, s)$ and that $m(s1_\Gamma + h1_y) - m(s1_\Gamma)$ is the measure of $\mathrm{cap}_\Gamma(y, s, h)$. Indeed,

$$\mathrm{Vol}_\mu(M(y, s+h) \cup M(\Gamma, s)) = \mathrm{Vol}_\mu(\mathrm{cap}_\Gamma(y, s, h)) + \mathrm{Vol}_\mu(M(\Gamma, s)).$$

Analogously, $m(s1_\Gamma + r1_z + h1_y) - m(s1_\Gamma + r1_z)$ is the measure of

$$M(y, s+h) \setminus (M(\Gamma, s) \cup M(z, s+r)) = \mathrm{cap}_\Gamma(y, s, h) \setminus M(z, s+r).$$

If $d(z, \mathrm{cap}_\Gamma(y, s, h)) < s + r$ then the intersection of $\mathrm{cap}_\Gamma(y, s, h)$ and $M(z, s+r)$ has strictly positive measure, whence (15) holds.

On the other hand, if $d(z, \mathrm{cap}_\Gamma(y, s, h)) \geq s + r$ then $\mathrm{cap}_\Gamma(y, s, h) \cap M(z, s+r)$ is contained in the topological boundary of $M(z, s+r)$ which is of zero measure [28]. Thus

$$m(s1_\Gamma + r1_z + h1_y) - m(s1_\Gamma + r1_z) = m(s1_\Gamma + h1_y) - m(s1_\Gamma),$$
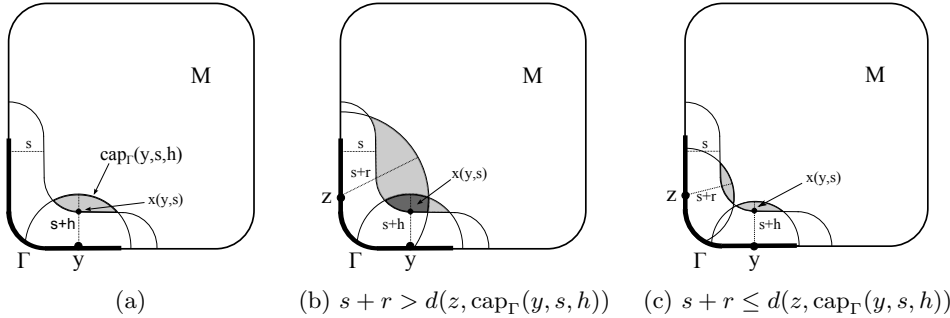
and (15) does not hold. □

Fig. 2: (a) A wave cap. (b)-(c) The light gray regions indicate the wave caps used in Lemma 4 and the dark gray region indicates the overlap between the caps.

The next lemma demonstrates that when $s < \sigma_\Gamma(y)$, the wave caps $\mathrm{cap}_\Gamma(y, s, h)$ tend, in a set-theoretic sense, towards $x(y, s)$.

LEMMA 5. *Let $y \in \Gamma$ and $s \in (0, \sigma_\Gamma(y))$. Then,*

$$\tag{16} \bigcap_{h>0} \mathrm{cap}_\Gamma(y, s, h) = \{x(y, s)\}.$$

Proof. Let y, s as above, and let $I(y, s)$ denote the left hand side of (16). Let w be any point belonging to $I(y, s)$. Then $w \in \mathrm{cap}_\Gamma(y, s, h)$ for all $h > 0$, so $s \leq d(\Gamma, w)$ and $d(y, w) < s + h$ for all $h > 0$, thus $d(y, w) \leq s$. Since $y \in \Gamma$, we conclude $s = d(\Gamma, w) = d(y, w)$. On the other hand, if w is a point in M satisfying $s = d(\Gamma, w) = d(y, w)$, then $w \in \mathrm{cap}_\Gamma(y, s, h)$ for any $h > 0$, hence $w \in I(y, s)$. We conclude,

$$\tag{17} I(y, s) = \{w \in M : d(y, w) = d(\Gamma, w) = s\}.$$

Because $s < \sigma_\Gamma(y)$, we have $d(x(y,s),y) = d(x(y,s),\Gamma) = s$, so $x(y,s) \in I(y,s)$. It remains to show that no other points belong to $I(y,s)$.

Let w belong to $I(y,s)$, we will show that $w = x(y,s)$. If we knew for certain that w belonged to the image of the semi-geodesic coordinates, then this would be immediate from the definition of these coordinates. On the other hand, if we did not require Γ to be open, then simple examples show that for points y in the topological boundary of Γ it is possible that $I(y,s)$ has many points. We demonstrate that when Γ is open this cannot happen.

Since M is a compact connected metric space with distance arising from a length function, the Hopf-Rinow theorem for length spaces applies and we conclude that there is a minimizing path $\beta : [0,l] \to M$ from y to w. By [2], β is C^1 and we may assume that it is unit speed parameterized. Hence $l = s$. As β is minimizing from both y and Γ to w, we see that $\dot\beta(0) = \nu$. Thus β coincides with $x(y,t)$ for $t \leq \min(s, \tau_M(y,\nu))$. But $s < \sigma_\Gamma(y)$, hence $s < \tau_M(y,\nu)$. Thus we see that $w = \beta(s) = x(y,s)$. $\qquad\square$

We use the preceding lemma to show that, when h is small, the distance between a point $z \in \Gamma$ and the wave cap $\mathrm{cap}_\Gamma(y,s,h)$ surrounding $x(y,s)$ yields an approximation to $d(z, x(y,s))$.

LEMMA 6. *For $y, z \in \Gamma$, and $s < \sigma_\Gamma(y)$, $d(z, \mathrm{cap}_\Gamma(y,s,h)) \to d(z, x(y,s))$ as $h \to 0$.*

Proof. Let $\{h_j\} \subset \mathbb{R}_+$ be a sequence for which $h_j \downarrow 0$. Then each $\mathrm{cap}_\Gamma(y,s,h_j)$ is compact, so there exists $w_j \in \mathrm{cap}_\Gamma(y,s,h_j)$ such that $d(z,w_j) = d(z, \mathrm{cap}_\Gamma(y,s,h_j))$. Because M is a compact manifold, the sequence $\{w_j\}$ has a convergent subsequence $\{w_{j_k}\}$ converging to a point w. Since the wave caps $\mathrm{cap}_\Gamma(y,s,h)$ nest, the tail of $\{w_{j_k}\}$ belongs to the closed set $\mathrm{cap}_\Gamma(y,s,h_{j_k})$ for each j_k, hence $w \in \mathrm{cap}_\Gamma(y,s,h)$ for each $h > 0$. By the previous lemma, we conclude $w = x(y,s)$.

Together, continuity of the distance function and the particular choice of the w_{j_k} imply that, $d(z, \mathrm{cap}_\Gamma(y,s,h_{j_k})) = d(z, w_{j_k}) \to d(z, x(y,s))$. Since the wave caps nest, the sequence $\{d(z,w_j)\}$ is monotone non-decreasing, and since it is bounded above it has a limit. In particular, any subsequential limit coincides with the limit. Thus we conclude that $d(z, \mathrm{cap}_\Gamma(y,s,h_j)) \to d(z, x(y,s))$ as $j \to \infty$, and in turn, $d(z, \mathrm{cap}_\Gamma(y,s,h)) \to d(z, x(y,s))$ as $h \to 0$. $\qquad\square$

The volumes appearing in Lemma 4 cannot be computed directly with the τ's appearing in the regularized volume determination. That is, the lemma requires us to compute volumes such as $m(s1_\Gamma + r1_z + h1_y)$, but the function $\tau = s1_\Gamma + r1_z + h1_y$ is equivalent to $s1_\Gamma$ in $L^2((0,T) \times \Gamma)$. As a result, the set $L^2(S_\tau)$ will produce waves that fill $L^2(M(s1_\Gamma))$ as opposed to the desired set $L^2(M(\tau))$. The problem is that the spikes $h1_y$ and $r1_z$ have supports with dS_g measure zero. The remedy is to replace the spikes by functions that produce the same domains of influence but have better supports. To accomplish this, for $y \in \Gamma$ and $R \in [0,\infty)$, we define τ_y^R on Γ by:

$$(18) \qquad\qquad \tau_y^R(z) := R - d(z,y) \quad \text{for } z \in \Gamma.$$

Note that τ_y^R is continuous. We recall that under Assumption 2 the distances $d(y,z)$ for $y, z \in \Gamma$ with $d(y,z) < T$ are known (or, alternatively, that they have been computed in some other fashion from Λ_Γ^{2T}). Thus under our assumptions the functions τ_y^R are known.

LEMMA 7. *Let $y, z \in \Gamma$, $s, r, h > 0$. We will use the notation $f \vee g$ to denote the function obtained by taking the pointwise maximum of f and g. Then, we have the*

following equalities,

$$(19) \qquad M(\tau_y^r) = M(r1_y),$$

$$(20) \qquad M(\tau_y^{s+h} \vee \tau_z^{s+r} \vee s) = M(h1_y + r1_z + s1_\Gamma),$$

$$(21) \qquad M(\tau_z^{s+r} \vee s) = M(s1_\Gamma + r1_z).$$

Proof. Let $x \in M(r1_y)$, then $d(y, x) < r$. Since $\tau_y^r(y) = r$, we have that $d(y, x) < \tau_y^r(x)$, hence $x \in M(\tau_y^r)$. Now let $x \in M(\tau_y^r)$. Then there is a point $z \in \Gamma$ for which $d(x, z) < \tau_y^r(z)$. Applying the definition of τ_y^r, we find $r > d(x, z) + d_\Gamma(y, z) \geq d(x, z) + d(y, z) \geq d(x, y)$. Hence $x \in M(r1_y)$. We conclude that $M(\tau_y^r) = M(r1_y)$.

We demonstrate equality (20) and note that (21) is proved in an analogous fashion. Let $\tau = \tau_y^{s+h} \vee \tau_z^{s+r} \vee s$. Then $x \in M(\tau)$ just in case $d(x, p) < \tau(p)$ for some $p \in \Gamma$, which happens if and only if $d(x, p)$ is less than $\tau_y^{s+h}(p), \tau_z^{r+h}(p)$, or s. The preceding paragraph implies that this happens just in case x belongs to $M((s + h)1_y), M((s + r)1_z)$, or $M(s1_\Gamma)$, which happens if and only if $x \in M(s1_y + r1_z + s1_\Gamma)$. $\qquad\square$

We are finally in a position to prove Theorem 1.

Proof (Of Theorem 1). First, let r and h be positive numbers satisfying $s+r < T$ and $s+h < T$. Define functions $\tau_1 = s$, $\tau_2 = \tau_y^{s+h} \vee s$, $\tau_3 = \tau_z^{s+r} \vee s$, and $\tau_4 = \tau_y^{s+h} \vee \tau_z^{s+r} \vee s$. Using the regularized volume determination from equation (14), we compute the volumes $m(\tau_i)$ for $i = 1, \ldots, 4$. Then, Lemma 7 implies that $m(\tau_1) = m(s1_\Gamma)$, $m(\tau_2) = m(s1_\Gamma + h1_y)$, $m(\tau_3) = m(s1_\Gamma + r1_z)$, and $m(\tau_4) = m(s1_\Gamma + h1_y + r1_z)$, thus we have determined the volumes appearing in (15). By Lemma 4 we can compute $d(z, \mathrm{cap}_\Gamma(y, s, h))$ by

$$(22) \qquad d(z, \mathrm{cap}_\Gamma(y, s, h)) = s + \inf\{r : 0 \leq r < T - s, \text{ and } (15) \text{ holds}\}.$$

Finally, by Lemma 6, we can compute $d(z, x(y, s))$ by

$$(23) \qquad d(z, x(y, s)) = \lim_{h \to 0} d(z, \mathrm{cap}_\Gamma(y, s, h)). \qquad\square$$

4.2. Alternative distance determination method. The method to determine distances derived from Theorem 1 uses the fact that, under the hypotheses of the theorem, the distance between a point $z \in \Gamma$ and the wave cap $\mathrm{cap}_\Gamma(y, s, h)$ serves as an approximation to $d(z, x(y, s))$, and that this approximation improves as $h \to 0$. However, in the case where g is the Euclidean metric, $d(z, \mathrm{cap}_\Gamma(y, s, h))$ converges to $d(z, x(y, s))$ with the rate $\mathcal{O}(h^{1/2})$. Thus the convergence is typically slow. In this section, we provide another technique to determine the distance to points which we find, for a given nonzero h, tends to provide better distance estimates.

The idea of this alternative distance determination method is to once again check for overlap between the sets $\mathrm{cap}_\Gamma(y, s, h)$ and $\mathrm{cap}_\Gamma(z, s, r)$, but instead of seeking the minimum r for which these wave caps overlap, we seek r for which $\mathrm{Vol}_\mu(\mathrm{cap}_\Gamma(y, s, h) \cap \mathrm{cap}_\Gamma(z, s, r))$ is half of $\mathrm{Vol}_\mu(\mathrm{cap}_\Gamma(y, s, h))$.

Before proving that our alternative distance determination procedure is valid, we provide a lemma that shows that the diameter of a wave cap vanishes as the height of the cap goes to zero.

LEMMA 8. *Let $y, z \in \Gamma$, $s \in (0, \sigma_\Gamma(y))$. Then,*

$$(24) \qquad \lim_{h \to 0} \mathrm{diam}(\mathrm{cap}(y, s, h)) = 0.$$

Proof. Suppose the claim were false. Then there exists a sequence of positive real numbers $h_i \downarrow 0$ and points $p_i \in \text{cap}_\Gamma(y, s, h_i)$ such that $d(x(y, s), p_i) \not\to 0$. Since M is compact, the sequence $\{p_i\}$ has a convergent subsequence. Relabeling this subsequence by p_i we have that there exists $p \in M$ such that $p_i \to p$. But this implies that $d(p, x(y, s)) \neq 0$, hence $p \neq x(y, s)$. On the other hand, since $p_i \in \text{cap}_\Gamma(y, s, h_i)$ we must have that $p \in \bigcap_{h>0} \text{cap}_\Gamma(y, s, h)$, but this gives a contradiction, since by Lemma 5 this implies that $p = x(y, s)$. $\square$

We now present our alternative distance determination method.

LEMMA 9. *Let* $y, z \in \Gamma$, $s \in (0, \sigma_\Gamma(y))$, *and* $0 < h < \sigma_\Gamma(y) - s$. *Let* r_h *be the solution to,*

$$(25) \qquad \text{Vol}_\mu(\text{cap}_\Gamma(y, s, h) \cap \text{cap}_\Gamma(z, s, r_h)) = \frac{1}{2} \text{Vol}_\mu(\text{cap}_\Gamma(y, s, h)).$$

Then, for $d_h := s + r_h$, *we have that* $d_h \to d(z, x(y, s))$ *as* $h \to 0$.

Proof. First, we recall that for s and h as above, $\text{cap}_\Gamma(y, s, h)$ will contain a non-empty open set, hence the right-hand side of (25) will be nonzero. Thus, from the definition of r_h, we conclude that $\text{cap}_\Gamma(y, s, h) \cap \text{cap}_\Gamma(z, s, r_h)$ is a non-empty and proper subset of $\text{cap}_\Gamma(y, s, h)$. Using the definition of $\text{cap}_\Gamma(z, s, r_h)$ and r_h we conclude that $s + r_h \geq d(z, \text{cap}_\Gamma(y, s, h))$. On the other hand, since the intersection between the wave caps is a proper subset of $\text{cap}_\Gamma(y, s, h)$ we see that there exists $p \in \text{cap}_\Gamma(y, s, h) \setminus \text{cap}_\Gamma(z, s, r_h)$. In particular, this implies that $s + r_h \leq d(z, p) \leq \text{dist}(z, \text{cap}_\Gamma(y, s, h)) + \text{diam}(\text{cap}_\Gamma(y, s, h))$. Hence,

$$d(z, \text{cap}_\Gamma(y, s, h)) \leq d_h \leq d(z, \text{cap}_\Gamma(y, s, h)) + \text{diam}(\text{cap}_\Gamma(y, s, h)).$$

Since $d(z, \text{cap}_\Gamma(y, s, h)) \to d(z, x(y, s))$ and $\text{diam}(\text{cap}_\Gamma(y, s, h)) \to 0$ as $h \to 0$, we conclude that $d_h \to d(z, x(y, s))$ as $h \to 0$. $\square$

We summarize the steps of the proof in an algorithmic form in Algorithm 1.

Algorithm 1 Continuum level distance determination using the alternate procedure.

Let: $y, z \in \Gamma$ and $s > 0$ with $r_{x(y,s)}(z) < T$.
Let: $h_0 > 0$ small enough that $s + h_0 < \min\{\sigma_\Gamma(y), T\}$.
for all $0 < h < h_0$:
    for all $0 < r < T - s$:
        Let: $\tau_1 = s1_\Gamma$, $\tau_2 = \tau_y^{s+h}$, $\tau_3 = \tau_z^{s+r}$, $\tau_4 = \tau_1 \vee \tau_2 \vee \tau_3$
        for all $\alpha > 0$:
            for $i = 1, \ldots, 4$:
                Let: $f_{\alpha,i}$ be the solution to $(K_{\tau_i} + \alpha)P_{\tau_i}f = P_{\tau_i}b$
        for $i = 1, \ldots, 4$:
            Compute: $m(\tau_i) = \lim_{\alpha \to 0}\langle f_{\alpha,i}, b\rangle_{L^2(S_\tau; dt \otimes dS_{g,\mu})}$
        Compute: $m_{\text{target cap}}(h) := m(\tau_2) - m(\tau_1)$
        Compute: $m_{\text{overlap}}(h, r) := m(\tau_4) - m(\tau_3) - m(\tau_2) + m(\tau_1)$
    Let: $r = r_h$ solve $m_{\text{overlap}}(h, r) = \frac{1}{2}m_{\text{target cap}}(h)$.
Compute: $r_{x(y,s)}(z) = s + \lim_{h \to 0} r_h$.

---

5. Computational experiments. In this section we present computational experiments demonstrating the distance determination procedure we have described in

the previous sections. We demonstrate our procedure in both Euclidean and hyperbolic geometries. However, we stress that our method can be applied in the general Riemannian setting.

5.1. Numerical method for the direct problem. In our computational experiments, we take M to be the 2-dimensional lower half-space $M = \{(x, y) : y \leq 0\}$ equipped with a conformally Euclidean metric $g = c^{-2}dx^2$. We consider the Euclidean case where $c \equiv 1$ and the hyperbolic case where $c = 1/(1 - y)$. In both cases, our weight is given by $\mu = c^{n-2}$, so the weighted Laplace-Beltrami operator that we consider is $c^{-2}\Delta$, where Δ denotes the 2-dimensional Euclidean Laplacian. Hence, in our experiments, the Riemannian wave equation (1) simplifies to the standard $2 + 1$-dimensional wave equation with wave speed c. In order to simulate partial data, for our source/receiver set, Γ, we take $\Gamma = [-L, L] \times \{0\} \subset \partial M$ with $L = 2.05$. We simulate waves propagating for $2T$ time units, where $T = 1.25$.

For sources, we use a basis of Gaussian pulses of the form

$$\varphi_{i,j}(t, x) = C \exp\left(-a_t(t - t_{s,i})^2 - a_x(x - x_{s,j})^2\right),$$

with parameters $a_t = a_x = 5.562 \cdot 10^3$, and we choose C to normalize the $\varphi_{i,j}$ in $L^2([0, T] \times \Gamma, dt \otimes dS_g)$. Sources are applied at regularly spaced points $(x_{s,j}, 0)$ with $x_{s,j} = -2 + (j - 1)\Delta x_s$ for $j = 1, \ldots, N_{x,s}$ and times $t_{s,i} = 0.05 + (i - 1)\Delta t_s$ for $i = 1, \ldots, N_{t,s}$. The source offset Δx_s and time between source applications Δt_s are both set as $\Delta x_s = \Delta t_s = .0125$. At each of the $N_{x,s} = 321$ source positions we apply $N_{t,s} = 93$ sources. For each basis function, we record the Dirichlet trace data at regularly spaced points $(x_{r,k}, 0)$ with $x_{r,k} = -2.05 + (k - 1)\Delta x_r$ for $k = 1, \ldots, N_{x,r}$ and times $t_{r,l} = (l - 1)\Delta t_r$ for $l = 1, \ldots, N_{t,r}$. The receiver offset Δx_r, satisfies $\Delta x_r = 0.5\Delta x_s$ resulting in $N_{x,r} = 657$ receiver positions. The time between receiver measurements, Δt_r, satisfies $\Delta t_r = 0.1\Delta t_s$, resulting in $N_{t,r} = 2001$ measurements at each receiver position.

We discretize the Neumann-to-Dirichlet map by solving the forward problem for each source $\varphi_{i,j}$ and recording its Dirichlet trace at the receiver positions and times described above. That is, we simulate the following data,

$$(26) \qquad \left\{ \Lambda^{2T}\varphi_{i,j}(t_{r,l}, x_{r,k}) = u^{\varphi_{i,j}}(t_{r,l}, x_{r,k}) : \begin{array}{l} i = 1, \ldots, N_{t,s}, \ j = 1, \ldots, N_{x,s}, \\ l = 1, \ldots, N_{t,r}, \ k = 1, \ldots, N_{x,r} \end{array} \right\}.$$

To perform the forward modelling, we use a continuous Galerkin finite element method with piecewise linear Lagrange polynomial elements and implicit Newmark time-stepping. In particular, we use the FEniCS package [25]. We use a regular triangular mesh, where the time step and mesh spacing are selected so that 8 points per wavelength (in directions parallel to the grid axes) are used at the frequency f_0 where the spectrum of the temporal portion of the source falls below 10^{-6} times its maximum value.

5.2. Solving the control problem. We discretize the connecting operator K by approximating its action as an operator on $\text{span}\{\varphi_{i,j}\}$. That is, we use the discrete Neumann-to-Dirichlet data, (26), to discretize K_τ by formula (6), where $\tau \equiv T$. To be specific, we first compute the Gram matrix $[G]_{ij} = \langle \varphi_i, \varphi_j \rangle_{L^2([0,T] \times \Gamma, dt \otimes dS_g)}$ and its inverse $[G^{-1}]$. Then, for $A = J\Lambda_\Gamma^{2T}$, $R\Lambda_\Gamma^T$ and RJ, we compute the matrix for A acting on $\text{span}\{\varphi_{i,j}\}$ by:

$$[A]_{ij} = \sum_k [G^{-1}]_{ik} \langle \varphi_k, A\varphi_j \rangle_{L^2([0,T] \times \Gamma, dt \otimes dS_g)}.$$

Finally, we use these matrices to compute the matrix for K:

$$(27) \qquad [K] = [J\Lambda_\Gamma^{2T}] - [R\Lambda_\Gamma^T][RJ].$$

For $\tau \in C(\Gamma)$, with $0 \le \tau \le T$, we obtain the matrix $[K_\tau]$ discretizing the connecting operator K_τ by masking the entries in $[K]$ that correspond to basis functions $\varphi_{i,j}$ with centers $(t_{s,i}, x_{s,j}) \notin S_\tau$. We note that, in practice, we find that this tends to provide a better approximation to K_τ than computing the matrix $[P_\tau]$ and computing the product $[P_\tau][K][P_\tau]$.

We consider the discretized control problem

$$(28) \qquad ([K_\tau] + \alpha[P_\tau])[f_\alpha] = [P_\tau][b],$$

where we use the matrix $[P_\tau]$ to refer to the mask described above, and use $\alpha = 10^{-5}$. Here, $[b]$ denotes the coefficient vector for the approximation to b in $\mathrm{span}\{\varphi_{ij}\}$ and we recall that $b(t, x) = T - t$, which was defined beneath (12). To solve (28) for $[f_\alpha]$, we use restarted GMRES. In Figure 3 and Table 1 we depict control solutions $f_\alpha = \sum_i [f_\alpha]_i \varphi_i$ and their associated wavefields $u^{f_\alpha}(T, \cdot)$. A volume estimate $\hat{m}(\tau)$ for $m(\tau)$ is obtained from $[f_\alpha]$ by computing the discretized inner product $\hat{m}(\tau) = [f_\alpha]^T[G][b]$, which approximates $m(\tau)$ as in (14). For the remainder of this paper we will continue to use the notation $\hat{m}(\tau)$ to indicate the approximation to $m(\tau)$ computed like this.
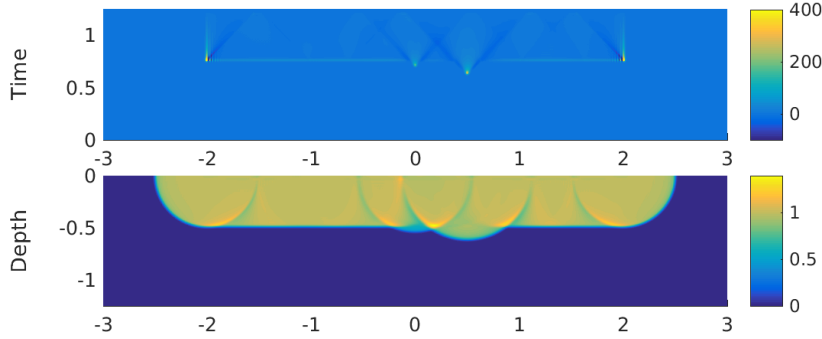

Fig. 3: Illustration, in the Euclidean case, of a source f_α (top) and the corresponding wavefield $u^{f_\alpha}(T, \cdot)$ (bottom) for which $u^{f_\alpha}(T, \cdot) \approx 1_{M(\tau)}$. Here, τ corresponds to τ_4 from Table 1. To show both plots with the same horizontal axis, we have extended f_α to zero outside of $[0, T] \times \Gamma$ and plotted time on the y-axis.

5.3. Estimating distances. We estimate distances between $z \in \Gamma$ and points of the form $x(y, s)$ where $y = (0, 0)$. In particular, for each fixed s we estimate the distances $d(x(y, s), (z_i, 0))$ for uniformly spaced $(z_i, 0) \in [-1, 1] \times \{0\} \subset \Gamma$. We take the offset Δz between the points z_i equal to $\Delta z = 4\Delta x_s = .05$, and select the points $(z_i, 0)$ to coincide with every fourth source position. As a proxy for estimating the distance to $x(y, s)$, we use a target wave cap of the form $\mathrm{cap}_\Gamma(y, s, h)$ with height $h = .025$, and estimate the distances $r_{x(y,s)}((z_i, 0))$ for $s = .125, .25, .375, .5$.

For each s we solve the discrete control problem (28) in order to obtain estimates $\hat{m}(s1_\Gamma)$ and $\hat{m}(\tau_y^{s+h})$ for the respective volumes of $M(\Gamma, s)$ and $M(y, s + h)$. From these, we estimate the volume of the target cap by,

$$\hat{m}_{\text{target cap}} = \hat{m}(\tau_y^{s+h}) - \hat{m}(s1_\Gamma).$$

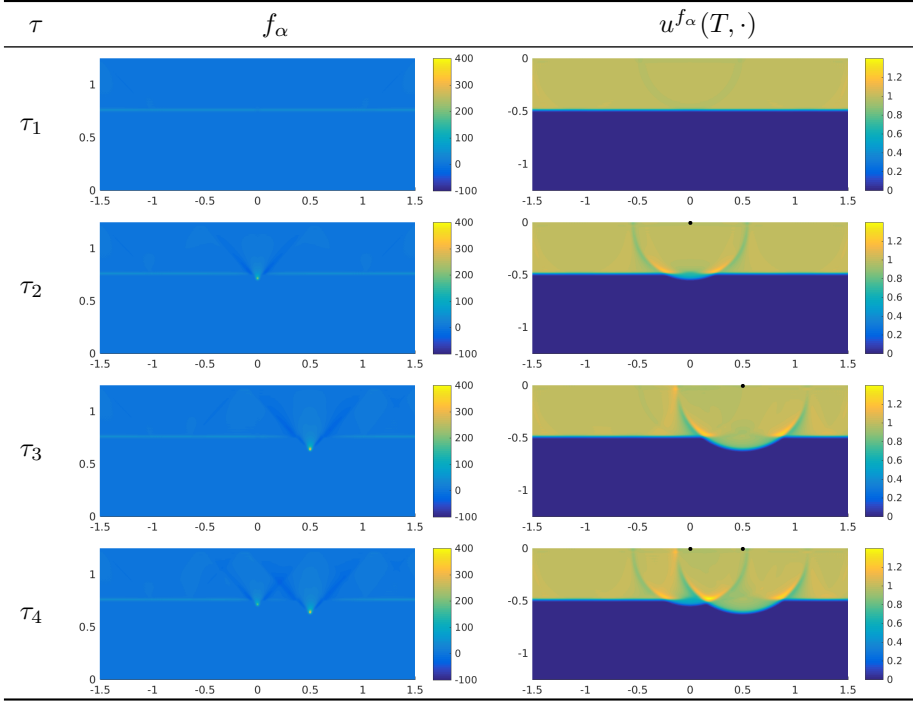| τ	f_α	$u^{f_\alpha}(T, \cdot)$
τ_1		
τ_2		
τ_3		
τ_4		

Table 1: Illustration, in the Euclidean case, of the essential features of sources and waves used in distance estimation procedure. See Figure 3 for interpretation of axes. Solutions, f_α, to the discretized control problem plotted next to their associated wavefields $u^{f_\alpha}(T, \cdot)$ approximating $1_{M(\tau)}$. Here, $\tau_1 = s1_\Gamma$, $\tau_2 = \tau_y^{s+h}$, $\tau_3 = \tau_z^{s+r}$, and $\tau_4 = \tau_1 \vee \tau_2 \vee \tau_3$, where $y = (0, 0)$, $z = (0.5, 0)$, $h = .05$, and $r = 0.125$. The black markers in the wavefield plots indicate the points y and z.

For each point $(z_i, 0)$, we also solve control problems to obtain volume estimates $\hat{m}(\tau_{(z_i,0)}^{r_j+s})$ and $\hat{m}(\tau_{(z_i,0)}^{r_j+s} \vee \tau_y^{s+h} \vee s1_\Gamma)$, where we select the parameters $r_j, j = 1, \ldots, N_r$ so that the two sets $\{s + r_j : j = 1, \ldots, N_r\} = \{t_{s,k} : t_{s,k} > r\}$ coincide. We implement the distance estimation procedure described in Lemma 9 to estimate $r_{x(y,s)}((z_i, 0))$ as follows: for each r_j we estimate $\text{Vol}_\mu(\text{cap}_\Gamma(y, s, h) \cap \text{cap}_\Gamma((z_i, 0), s, r_j))$ by,

$$\hat{m}_{\text{overlap},j} = \hat{m}(\tau_{(z_i,0)}^{r_j+s} \vee \tau_y^{s+h} \vee s1_\Gamma) - \hat{m}(\tau_{(z_i,0)}^{r_j+s}) - \hat{m}(\tau_y^{h+s}) + \hat{m}(s1_\Gamma).$$

We then find the indices $j, j + 1$ for which

$$(29) \qquad \hat{m}_{\text{overlap},j} \leq \frac{1}{2}\hat{m}_{\text{target cap}} \leq \hat{m}_{\text{overlap},j+1},$$

and estimate r_h by linearly interpolating between r_j and r_{j+1}. This procedure approximates (25). We depict the results of the volume overlap estimation in Figure 4. Since the volumes in these images have all been normalized by the target cap volumes, computing r_h by (29) corresponds to finding the x-value where the curve connecting the data points passes through the line $y = 0.5$. We depict the distance estimation results in Figure 5.
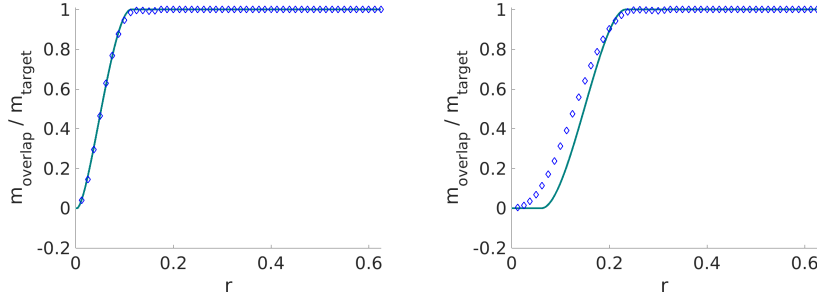
Fig. 4: Some examples, in the Euclidean case, of relative overlap volumes, $m_{\text{overlap}}/m_{\text{target cap}}$, vs. r. For $s = .25$, $h = .025$ and $z = 0.15$ (left) and $z = 0.3$ (right). The markers denote relative overlap volumes estimated in the distance estimation procedure, and the curves indicate analytical relative overlap volumes.
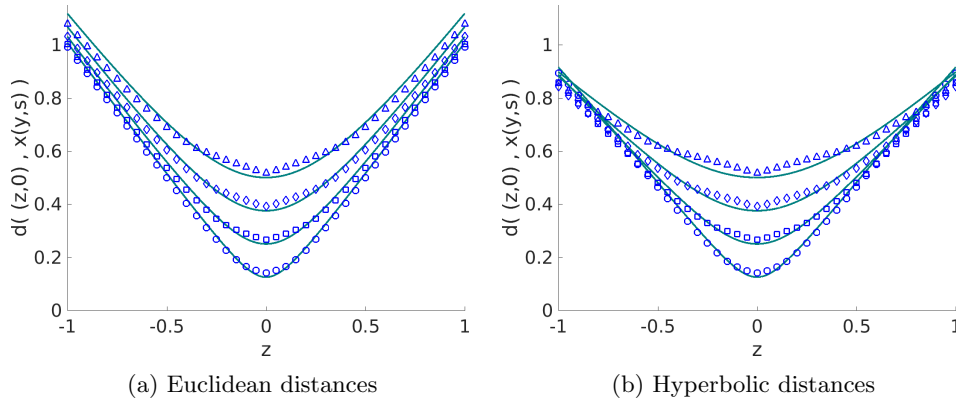

(a) Euclidean distances   (b) Hyperbolic distances

Fig. 5: Distance estimates (markers) for $d(x(y,s),(z_i,0))$ for $y = (0,0)$ and for $s = .125, .25, .375, .5$, plotted along with the true distances (solid curves).

5.4. Discussion of sources of numerical errors and instability. Examining Figure 5, one can see that in each of the estimated distance curves, the distances are over-estimated for $z = (z_i, 0)$ near $y = (0,0)$. This error results in part from the distance estimation method. For example, when $z = y$ the correct distance $d = s + r$ would be obtained by taking $r = 0$. On the other hand, when $z = y$, both of the wave caps used in the distance estimation procedure are centered on the same point, so for $0 \leq r \leq h$ the variable wave cap, $\text{cap}_\Gamma(z, s, r)$, coincides with $\text{cap}_\Gamma(z, s, r) \cap \text{cap}_\Gamma(y, s, h)$. From the definition of r_h, we find that we will have $0 < r_h < h$. Thus the distance estimate d_h will necessarily over-estimate $d(y, x(y,s))$. Similar remarks apply for estimating $d((z_i,0), x(y,s))$ for $(z_i, 0)$ near y, although the strength of this effect decreases as $(z_i, 0)$ gets further from y. We call this source of error *geometric distortion*, since it results entirely from the geometry of our distance estimation procedure and is independent of errors arising from the control problems. In Figure 6 we depict the geometric distortion by repeating our distance estimation technique with exact volume measurements. Note that the distances in Figure 6 are

overestimated at all points, which contrasts most with the distances estimated at large offsets in Figure 5.
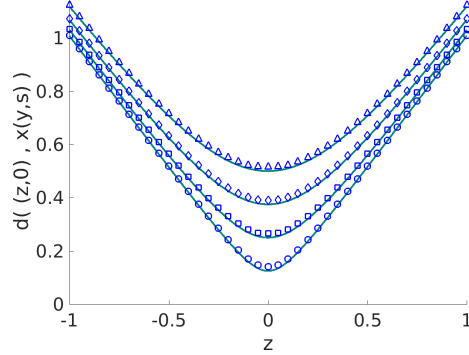

Fig. 6:   Demonstration of geometric distortion in the Euclidean case. Distances (markers) are estimated by using the distance estimation technique on exact volumes and plotted for $d(x(y, s), (z_i, 0))$ for $y = (0, 0)$ and $s = .125, .25, .375, .5$, along with the true distances (solid curves).

Our numerical tests suggest that the dominant source of error comes from the control step. In order to discuss this instability, we return to considering the continuum problem. Taking $\tau \in C(\overline{\Gamma})$, we can ask whether there exists $f \in H^s(S_\tau)$ for some $s \in \mathbb{R}$ for which $W_\tau f = 1_{M(\tau)}$. This question can be answered by considering the more general problem of exact controllability, in which one seeks to determine when the equation $(u^f(T, \cdot), \partial_t u^f(T, \cdot)) = (w_0, w_1)$ has a solution in $H^s(S_\tau)$ for any (w_0, w_1) belonging to an appropriate space of Cauchy data for the wave equation.

In [4], the question of exact controllability is considered. One of the main results of that paper is that the ray geometry of the wave equation can be used to determine necessary and sufficient conditions for exact controllability. Using the same set of ideas to those in [4], it is shown in [3] that in order for exact controllability to hold for W_τ in $M(\tau)$ from S_τ, the following *geometric controllability condition* must hold:

Each generalized bicharacteristic $(x(t), t)$ satisfying $x(T) \in M(\tau)$, passes over $S_\tau \cup S_\tau'$ in a non-diffractive point.

Here, $S_\tau' = \{(t, x) \in \Gamma \times (T, 2T) : T \leq t \leq T + \tau(x)\}$. We recall that S_τ is defined by (3), and note that S_τ' is the temporal reflection of S_τ across $t = T$. For a generalized bicharacteristic $(x(t), t)$, the path $x(t)$ is a unit speed geodesic in the interior of M and it is reflected according to Snell's law when it intersects the boundary ∂M transversally. Tangential intersections with the boundary can cause the path to glide along the boundary, and in the case of an infinite-order contact, the path $x(t)$ can be continued in many ways, see [4]. We refer also to [4] for the definition of non-diffractive points. The geometric controllability condition is necessary for exact control to hold from S_τ, since when it fails for $(x, \xi) \in S^*(M(\tau))$, propagation of singularities implies that for any $s \in \mathbb{R}$ and any $f \in H^s(S_\tau)$, $(x, \xi) \notin \mathrm{WF}(u^f(T, \cdot))$, see e.g. [15, Section 23]. Here, $\mathrm{WF}(u^f(T, \cdot))$ denotes the wave front set of $u^f(T, \cdot)$, and we refer to [16, Def. 8.1.2] for its definition. Thus, if $w \in L^2(M(\tau))$ has $(x, \xi) \in \mathrm{WF}(w)$ then, for each $s \in \mathbb{R}$, there does not exist $f \in H^s(S_\tau)$ for which $W_\tau f = w$.

In our computational experiments, the geometric controllability condition actually fails over every point in $M(\tau)$. This is due to the fact that at each $x \in M(\tau)$ there

exists a family of unit-speed geodesic rays with $(\gamma(T), \dot{\gamma}(T)) = (x, \xi) \in S_x(M)$ and ξ belonging to a cone over x, for which the corresponding geodesics γ fail to pass over $S_\tau \cup S'_\tau$. For an approximate control solution $u^f(T, \cdot)$ approximating $1_{M(\tau)}$, we observe instabilities near $x \in M(\tau)$ where $\mathrm{WF}(1_{M(\tau)})$ meets the cone over which exact control fails. In particular, for the τ considered in our experiments, $\mathrm{WF}(1_{M(\tau)})$ meets the uncontrollable cone only above points $x \in \partial M(\tau)$ where $\partial M(\tau)$ fails to be C^∞ smooth. Above all other points, $\mathrm{WF}(1_{M(\tau)})$ is either empty or only contains controllable directions. We note that for those points x where $\partial M(\tau)$ fails to be smooth, $\{x\} \times (\mathbb{R}^2 \setminus 0) \subset \mathrm{WF}(1_{M(\tau)})$, and refer to Appendix A for further analysis.
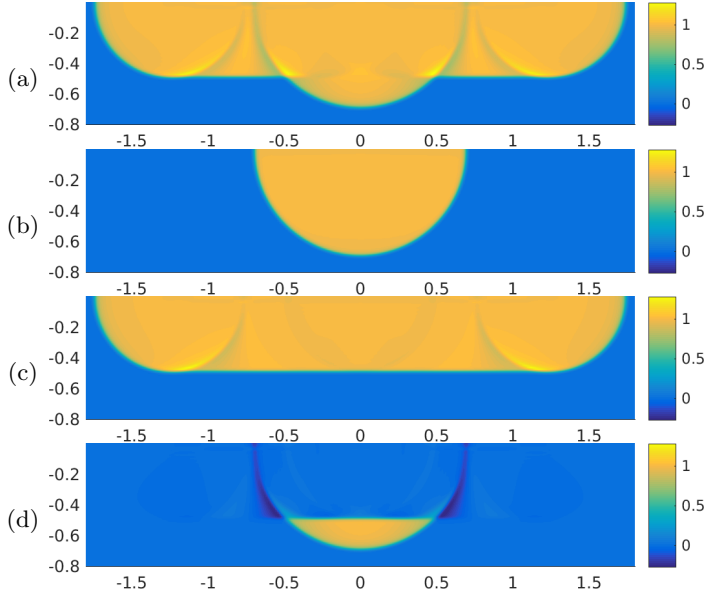

Fig. 7: (a) A wavefield demonstrating instability of the solution to the control problem when $\mathrm{WF}(1_{M(\tau)})$ contains uncontrollable directions over $(\pm.5, -.5)$ and $(\pm 1.25, -.5)$ (b) A wavefield for which all directions in $\mathrm{WF}(1_{M(\tau)})$ are controlled. (c) Another wavefield demonstrating instability, with uncontrollable directions in $\mathrm{WF}(1_{M(\tau)})$ over $(\pm 1.25, -.5)$. (d) The difference between the wavefields (a) and (c). Note that this corresponds to an approximation to $1_{\mathrm{cap}(y,s,h)}$. Moreover, the instabilities in (a) and (c) located over $(\pm 1.25, -.5)$ appear to cancel each other.

In the case of $\tau = \tau_y^{s+h} \vee s1_\Gamma$, instabilities occur for x in the corners of $\mathrm{cap}_\Gamma(y, s, h)$, where $\partial M(\tau)$ fails even to be C^1. Additionally, we observe instabilities near the points $(\pm L, -s)$, where the flat portion of $\partial M(\tau)$ transitions into a circle and fails to be C^2. We demonstrate these effects in Figure 7a, by plotting a wavefield $u^f(T, \cdot)$ approximating $1_{M(\tau)}$ for $y = (0,0), s = .5$, and $h = .2$. The former instabilities occur near the points $(\pm.5, -.5)$, and the latter instabilities occur near $(\pm 1.25, -.5)$. We contrast this with the case where $\tau = \tau_y^{s+h}$, which we show in Figure 7b. In this second example, the domain of influence is a disk and every co-vector in $\mathrm{WF}(1_{M(\tau)})$ can be controlled, and unlike the first example, we observe no instabilities. Note that in all of the examples in Figure 7 we restrict our computations to $\Gamma = [-1.25, 1.25]$.

In Figure 7c we plot the wavefield $u^f(T, \cdot)$ that approximates $1_{M(s1_\Gamma)}$. Note that as in the case of $\tau = \tau_y^{s+h} \vee s1_\Gamma$, we observe instabilities near the points $(\pm 1.25, -.5)$.

In Figure 7d we plot the difference between the wave fields approximating $1_{M(\tau_y^{s+h} \vee s1_\Gamma)}$ and $1_{M(s1_\Gamma)}$, and note that this difference yields an approximation to the characteristic function of $\text{cap}_\Gamma(y, s, h)$. In particular, we note that the instabilities observed near $(\pm 1.25, -.5)$ in Figures 7a and 7c appear to cancel upon taking the difference in Figure 7d. On the other hand, instabilities near the corners of the caps at $(\pm.5, -.5)$ persist after taking the difference. Since our distance determination procedure relies primarily on the volumes of wave caps, which are obtained by taking differences in this fashion, we find that the instabilities near the corners of the caps tend to provide the main source of error for our distance estimation procedure.

Appendix A. Wave front set of $1_{M(\tau)}$. In Section 5 all of the functions τ that we consider give rise to sets $M(\tau)$ with piecewise smooth boundary. For these functions, if $x \in \partial M(\tau)$ is a point at which $\partial M(\tau)$ is not smooth, then $\partial M(\tau)$ either fails to be C^1 or C^2 at x. We compute the wave front set of $1_{M(\tau)}$ over a point x where $\partial M(\tau)$ fails to be C^1. In particular, we show that $\{x\} \times (\mathbb{R}^2 \setminus 0) \subset \text{WF}(1_{M(\tau)})$. Put differently, $\text{WF}(1_{M(\tau)})$ contains all cotangent directions above the point x. The case where $\partial M(\tau)$ fails to be C^2 at a point is similar and we omit it.

We begin by noting that if $h \in \mathbb{R}$, $u \in C_0^\infty(\mathbb{R})$, and $\phi \in C^\infty(\mathbb{R})$ is real valued and has no critical points in $\text{supp}(u)$, then:

$$(30) \quad \int_{-\infty}^{h} u(x) e^{-i\lambda\phi(x)} dx = \frac{iu(h) e^{-i\lambda\phi(h)}}{\lambda\phi'(h)} + \frac{\partial_x(u/\phi')|_{x=h} \, e^{-i\lambda\phi(h)}}{\lambda^2\phi'(h)} + \frac{R(\lambda, h, \phi, u)}{\lambda^3}.$$

Here, $|R|$ is bounded by a constant that depends only on $\text{supp}(u)$, $\min_{x \in \text{supp}(u)} |\phi'(x)|$ and the C^3 norms of u and ϕ. The proof of (30) follows from repeated integration by parts and the fact that for $L := i\phi'^{-1}\partial_x$, $Le^{-i\lambda\phi} = e^{-i\lambda\phi}$.

Since $\partial M(\tau)$ is assumed to be piecewise smooth with a discontinuous derivative at x, after a rotation and translation we may assume that $x = (0,0)$ and locally identify $M(\tau)$ with $A := \{(x^1, x^2) : x^2 \leq h(x^1)\}$ where $h : \mathbb{R} \to \mathbb{R}$ is smooth on $\mathbb{R} \setminus 0$, $h \notin C^1(\mathbb{R})$, and $h(0) = 0$. Thus, it will suffice show that $\{(0,0)\} \times (R^2 \setminus 0) \subset \text{WF}(1_A)$.

Let $u \in C_0^\infty(\mathbb{R}^2)$ with $u = 1$ near the origin. We consider the Fourier transform

$$\widehat{u1_A}(\lambda\xi) = \int_{-\infty}^{+\infty} e^{-i\lambda\xi_1 x^1} \int_{-\infty}^{h(x^1)} u(x) e^{-i\lambda\xi_2 x^2} dx^2 dx^1,$$

where ξ is a unit vector and $\lambda > 0$. First we suppose that $\xi_2 \neq 0$. Then by (30),

$$\int_{-\infty}^{h(x^1)} u(x) e^{-i\lambda\xi_2 x^2} dx^2 = \frac{iw(x^1) e^{-i\lambda\xi_2 h(x^1)}}{\lambda\xi_2} + \frac{v(x^1) e^{-i\lambda\xi_2 h(x^1)}}{\lambda^2\xi_2^2} + \frac{R}{\lambda^3},$$

where $w(x^1) = u(x^1, h(x^1))$ and $v(x^1) = \partial_{x^2} u(x^1, h(x^1))$. Note that R, w, and v are compactly supported with respect to x^1 since u is. Also note that $w = 1$ near $x^1 = 0$. If we choose u such that $\text{supp}(u)$ is small enough then h will be smooth in $(\text{supp}(w) \cup \text{supp}(v)) \setminus 0$. In particular, w and v are smooth away from 0.

We define $\phi(x^1) = \xi_1 x^1 + \xi_2 h(x^1)$, $\phi_\pm = \phi|_{\pm x^1 > 0}$, and define also $h_\pm$ analogously. Suppose that $\phi'_-(0) = \xi_1 + h'_-(0)\xi_2 \neq 0$. Then ϕ has no critical points in the set $\{x^1 < 0\} \cap \text{supp}(w)$ if $\text{supp}(w)$ is taken small enough. Thus by (30),

$$\int_{-\infty}^{0} w e^{-i\lambda\phi} dx^1 = \frac{i}{\lambda\phi'_-(0)} + \frac{R_+(\lambda, h, \phi, u)}{\lambda^2}.$$

A similar expression holds for the integral from 0 to ∞ if $\phi'_+(0) \neq 0$. Applying an analogous argument to v, we see that $\int_{-\infty}^{+\infty} v e^{-i\lambda\phi} dx^1 = \mathcal{O}(\lambda^{-1})$. Hence,

$$\widehat{u1_A}(\lambda\xi) = \frac{1}{\xi_2}\left(\frac{1}{\phi'_+(0)} - \frac{1}{\phi'_-(0)}\right)\lambda^{-2} + \mathcal{O}(\lambda^{-3}).$$

Thus $\widehat{u1_A}$ does not decay rapidly if $\phi'_+(0) \neq \phi'_-(0)$, equivalently if $h'_+(0) \neq h'_-(0)$.

To summarize, if $h'_+(0) \neq h'_-(0)$ then over the point $(0,0)$, $\mathrm{WF}(1_A)$ contains all directions except possibly $(1,0)$ and the four directions $(-h'_\pm(0)\xi^2, \xi^2)$, where $|\xi_2| = (|h'_\pm(0)|^2 + 1)^{-1/2}$. Finally, since a wave front set is a closed conic set [16], we conclude that $\{(0,0)\} \times (\mathbb{R}^2 \setminus 0) \subset \mathrm{WF}(1_A)$.

REFERENCES

[1] G. ALESSANDRINI, *Stable determination of conductivity by boundary measurements*, Appl. Anal., 27 (1988), pp. 153–172, doi:10.1080/00036818808839730.

[2] R. ALEXANDER AND S. ALEXANDER, *Geodesics in Riemannian manifolds-with-boundary*, Indiana University Math Journal, 30 (1981), pp. 481–488.

[3] C. BARDOS AND M. BELISHEV, *The wave shaping problem*, in Partial Differential Equations and Functional Analysis, J. Cea, D. Chenais, G. Geymonat, and J. Lions, eds., vol. 22 of Progress in Nonlinear Differential Equations and Their Applications, Birkhuser Boston, 1996, pp. 41–59, doi:10.1007/978-1-4612-2436-5_4.

[4] C. BARDOS, G. LEBEAU, AND J. RAUCH, *Sharp sufficient conditions for the observation, control, and stabilization of waves from the boundary*, SIAM J. Control Optim., 30 (1992), pp. 1024–1065.

[5] M. BELISHEV AND Y. Y. GOTLIB, *Dynamical variant of the BC-method: theory and numerical testing.*, Journal of Inverse & Ill-Posed Problems, 7 (1999), p. 221.

[6] M. I. BELISHEV, *An approach to multidimensional inverse problems for the wave equation*, Dokl. Akad. Nauk SSSR, 297 (1987), pp. 524–527.

[7] M. I. BELISHEV, *Boundary control in reconstruction of manifolds and metrics (the BC method)*, Inverse Problems, 13 (1997), pp. R1–R45, doi:10.1088/0266-5611/13/5/002.

[8] M. I. BELISHEV AND Y. V. KURYLEV, *To the reconstruction of a Riemannian manifold via its spectral data (BC-method)*, Comm. Partial Differential Equations, 17 (1992), pp. 767–804, doi:10.1080/03605309208820863.

[9] M. BELLASSOUED AND D. DOS SANTOS FERREIRA, *Stability estimates for the anisotropic wave equation from the Dirichlet-to-Neumann map*, Inverse Probl. Imaging, 5 (2011), pp. 745–773, doi:10.3934/ipi.2011.5.745.

[10] K. BINGHAM, Y. KURYLEV, M. LASSAS, AND S. SILTANEN, *Iterative time-reversal control for inverse problems*, Inverse Probl. Imaging, 2 (2008), pp. 63–81.

[11] A. S. BLAGOVESHCHENSKII, *The local method of solution of the nonstationary inverse problem for an inhomogeneous string*, Trudy Mat. Inst. Steklov., 115 (1971), p. 2838.

[12] A.-P. CALDERÓN, *On an inverse boundary value problem*, in Seminar on Numerical Analysis and its Applications to Continuum Physics, Soc. Brasil. Mat., Rio de Janeiro, 1980, pp. 65–73.

[13] M. DAHL, A. KIRPICHNIKOVA, AND M. LASSAS, *Focusing waves in unknown media by modified time reversal iteration*, SIAM Journal on Control and Optimization, 48 (2009), pp. 839–858.

[14] M. DE HOOP, S. HOLMAN, E. IVERSEN, M. LASSAS, AND B. URSIN, *Reconstruction of a conformally Euclidean metric from local boundary diffraction travel times*, SIAM Journal on Mathematical Analysis, 46 (2014), pp. 3705–3726, doi:10.1137/130931291.

[15] L. HÖRMANDER, *The analysis of linear partial differential operators. III*, vol. 274 of Grundlehren der Mathematischen Wissenschaften, Springer-Verlag, Berlin, 1985.

[16] L. HÖRMANDER, *The analysis of linear partial differential operators. I*, vol. 256 of Grundlehren der Mathematischen Wissenschaften, Springer-Verlag, Berlin, 1990.

[17] P. HUBRAL AND T. KREY, *Interval Velocities from Seismic Reflection Time Measurements*, Society of Exploration Geophysicists, 1980, doi:10.1190/1.9781560802501.

[18] S. I. KABANIKHIN, A. D. SATYBAEV, AND M. A. SHISHLENIN, *Direct methods of solving multidimensional inverse hyperbolic problems*, Inverse and Ill-posed Problems Series, VSP, Utrecht, 2005.

[19] A. KATCHALOV, Y. KURYLEV, AND M. LASSAS, *Inverse boundary spectral problems*, vol. 123 of Monographs and Surveys in Pure and Applied Mathematics, Chapman & Hall/CRC, Boca Raton, FL, 2001, doi:10.1201/9781420036220.

[20] A. KATSUDA, Y. KURYLEV, AND M. LASSAS, *Stability of boundary distance representation and reconstruction of Riemannian manifolds*, Inverse Problems and Imaging, 1 (2007), pp. 135–157, doi:10.3934/ipi.2007.1.135.

[21] A. KIRSCH, *An Introduction to the Mathematical Theory of Inverse Problems*, Springer, New York, 2011.

[22] I. LASIECKA AND R. TRIGGIANI, *Sharp regularity theory for second order hyperbolic equations of Neumann type. part 1. L_2 nonhomogeneous data*, Annali di Mathematica Pura ed Applicata, 157 (1990).

[23] M. LASSAS AND L. OKSANEN, *Inverse problem for the Riemannian wave equation with Dirichlet data and Neumann data on disjoint sets*, Duke Math. J., 163 (2014), pp. 1071–1103, doi:10.1215/00127094-2649534.

[24] S. LIU AND L. OKSANEN, *A Lipschitz stable reconstruction formula for the inverse problem for the wave equation*, Trans. Amer. Math. Soc. (to appear). Preprint arXiv:1210.1094, (2012).

[25] A. LOGG, K.-A. MARDAL, G. N. WELLS, ET AL., *Automated Solution of Differential Equations by the Finite Element Method*, Springer, 2012, doi:10.1007/978-3-642-23099-8.

[26] N. MANDACHE, *Exponential instability in an inverse problem for the Schrödinger equation*, Inverse Problems, 17 (2001), pp. 1435–1444, doi:10.1088/0266-5611/17/5/313.

[27] C. MONTALTO, *Stable determination of a simple metric, a covector field and a potential from the hyperbolic dirichlet-to-neumann map*, Communications in Partial Differential Equations, 39 (2014), pp. 120–145, doi:10.1080/03605302.2013.843429.

[28] L. OKSANEN, *Solving an inverse problem for the wave equation by using a minimization algorithm and time-reversed measurements*, Inverse Problems and Imaging, 5 (2011), pp. 731–744, doi:10.3934/ipi.2011.5.731.

[29] L. OKSANEN, *Inverse obstacle problem for the non-stationary wave equation with an unknown background*, Communications in Partial Differential Equations, 38 (2013), pp. 1492–1518, doi:10.1080/03605302.2013.804550.

[30] L. OKSANEN, *Solving an inverse obstacle problem for the wave equation by using the boundary control method*, Inverse Problems, 29 (2013), pp. 035004, 12, doi:10.1088/0266-5611/29/3/035004.

[31] L. PESTOV, V. BOLGOVA, AND A. DANILIN, *Numerical recovering of a speed of sound by the BC-method in 3D*, in Acoustical Imaging, A. Nowicki, J. Litniewski, and T. Kujawska, eds., vol. 31 of Acoustical Imaging, Springer Netherlands, 2012, pp. 201–209, doi:10.1007/978-94-007-2619-2_20.

[32] L. PESTOV, V. BOLGOVA, AND O. KAZARINA, *Numerical recovering of a density by the BC-method*, Inverse Probl. Imaging, 4 (2010), pp. 703–712, doi:10.3934/ipi.2010.4.703.

[33] L. PESTOV, G. UHLMANN, AND H. ZHOU, *An inverse kinematic problem with internal sources*, Inverse Problems, 31 (2015), p. 055006.

[34] P. STEFANOV AND G. UHLMANN, *Stability estimates for the hyperbolic Dirichlet to Neumann map in anisotropic media*, Journal of Functional Analysis, 154 (1998), pp. 330 – 358, doi:10.1006/jfan.1997.3188.

[35] P. STEFANOV AND G. UHLMANN, *Stable determination of generic simple metrics from the hyperbolic Dirichlet-to-Neumann map*, Int. Math. Res. Not., (2005), pp. 1047–1061, doi:10.1155/IMRN.2005.1047.

[36] P. STEFANOV, G. UHLMANN, AND A. VASY, *On the stable recovery of a metric from the hyperbolic DN map with incomplete data*, May 2015, arXiv:1505.02853.

[37] J. SYLVESTER AND G. UHLMANN, *A global uniqueness theorem for an inverse boundary value problem*, Ann. of Math. (2), 125 (1987), pp. 153–169, doi:10.2307/1971291.

[38] D. TATARU, *Unique continuation for solutions to pde's; between Hörmander's theorem and Holmgren's theorem*, Communications in Partial Differential Equations, 20 (1995), pp. 855–884, doi:10.1080/03605309508821117.

[39] D. TATARU, *On the regularity of boundary traces for the wave equation*, Ann. Scuola Norm. Sup. Pisa Cl. Sci. (4), 26 (1998), pp. 185–206.